

Surface Coating with Cyclic RGD Peptides Stimulates Osteoblast Adhesion and Proliferation as well as Bone Formation

Martin Kantlehner,^[a] Patricia Schaffner,^[b] Dirk Finsinger,^[a] Jörg Meyer,^[b] Alfred Jonczyk,^[c] Beate Diefenbach,^[c] Berthold Nies,^[b] Günter Hölzemann,^[c] Simon L. Goodman,^[c] and Horst Kessler*^[a]

The physiological inertness of synthetic implant materials often results in insufficient implant integration and limited acceptance of implants in tissues. After implantation the implant surface is often separated from the surrounding healthy and regenerating tissue, for example by a fibrous capsule. To avoid this host-versus-graft reaction, a strong mechanical contact between tissue and implant must be ensured. An enhanced contact between graft and the surrounding tissue can be provided by coating the implant with cell-adhesive molecules. The highly active and $\alpha_v\beta_3$ - and $\alpha_v\beta_5$ -integrin-selective peptide c(-RGDfK-) (f=D-phenylalanine) was functionalized with various linker molecules containing an acrylamide end group by using the lysine side chain of c(-RGDfK-). The acrylamide group can be used to bind the peptide covalently to poly(methyl methacrylate) (PMMA) surfaces. The coated surfaces effectively bind to murine osteoblasts as well as human osteoblasts

in vitro when a minimum distance of 3.5 nm between surface and the constrained RGD sequence is provided. In contrast to osteoblasts in cell suspension, surface-bound osteoblasts show no apoptosis but proliferate by a factor of 10 over a 22 d period. Coating of inert implant surfaces with highly active and α_v -selective peptides affords a marked improvement in osteoblast binding over current technologies. *In vivo* studies show that peptide-coated PMMA pellets implanted into the patella groove of rabbits are integrated into the regenerating bone tissue faster and more strongly than uncoated pellets.

KEYWORDS:

bioorganic chemistry · integrins · materials science · RGD peptides · surface chemistry

Introduction

Although most currently employed implant materials (polymers, carbon fibers, metals) are biocompatible, that is, nontoxic and stable against degradation in the organism, an insufficient integration into the surrounding tissue often occurs. Fibrous capsule formation and inflammation prevent the generation of a stable implant-to-tissue binding. Limited acceptance of materials in tissues is due to improper mechanical contact between implant surface and the cells of the regenerating tissue. In the case of bone implants, a strong mechanical contact between bone tissue produced by osteoblasts and the implant surface is required for integration.

Coating of implant surfaces with cell-adhesive molecules provides a strong mechanical contact between cells and the surface. Cell adhesion is mediated by integrins,^[1] a class of heterodimeric transmembrane cell receptors that bind selectively to different proteins of the extracellular matrix (ECM).^[2] Binding of ECM proteins often effects a signal transduction,^[3–7] for example, cell proliferation and apoptosis are two contrary effects that are both integrin-dependent. It is known that the cell types of different tissues express a different, cell-specific integrin pattern and that some cell types change their integrin pattern during their lifetime. The advantage of coating surfaces with ECM proteins such as fibronectin, vitronectin, or collagen^[8] is the

selectivity of these proteins towards specific integrin receptors. Therefore, certain cell types will selectively bind to their favorite ECM protein. Furthermore, ECM proteins do not cause any harmful side effects as they are the natural integrin ligands. The disadvantages, however, are: the difficulty of obtaining a stable attachment to the material, their immunogenicity, relatively high costs, large molecular weight, instability towards enzymatic degradation in the organism, as well as problems with sterilization.

Another approach to coating surfaces uses small peptides containing only the binding sequence of the natural protein ligands for surface coating.^[9–24] The advantage of using small

[a] Prof. Dr. H. Kessler, M. Kantlehner, Dr. D. Finsinger
Institut für Organische Chemie und Biochemie
Technische Universität München
Lichtenbergstrasse 4, 85747 Garching (Germany)
Fax: (+49) 89-289-13210
E-mail: kessler@ch.tum.de

[b] P. Schaffner, Dr. J. Meyer, Dr. B. Nies
Merck Biomaterial GmbH, Forschung
Frankfurter Strasse 250, 64271 Darmstadt (Germany)

[c] Dr. A. Jonczyk, B. Diefenbach, Dr. G. Hölzemann, Dr. S. L. Goodman
Merck KGaA, Präklinische Forschung
Frankfurter Strasse 250, 64271 Darmstadt (Germany)

peptides is the ease with which they can be synthesized and handled and their low immunogenic activity. On the other hand, small peptides often have lower binding activity and selectivity for distinct integrin subtypes. Linear peptides are also easily enzymatically cleaved. Over the last decade, highly active and $\alpha_v\beta_3$ - and $\alpha_v\beta_5$ -integrin-selective cyclic pentapeptide ligands such as c(-RGDFX-) have been developed.^[25–29] It has been demonstrated that in addition to the RGD binding sequence a D-amino acid, especially D-Phe following the Asp residue in the cyclus, is essential for high activities and α_v selectivities. Cyclic pentapeptides with D-amino acids in other positions and/or a nonhydrophobic amino acid following Asp as well as linear peptides have lower activity and are less selective towards α_v integrins.^[28, 29] Furthermore, the amino acid X in position 5 has no significant influence on the selectivity and activity of the peptides towards the $\alpha_v\beta_3$ and $\alpha_v\beta_5$ integrins. Therefore, c(-RGDFK-) was used as the ligand because this peptide can easily be functionalized through the ϵ -amino group of the lysine side chain. After preliminary studies of coating bovine serum albumin (BSA) surfaces by using thiol anchors, we aimed for a direct attachment of the peptides to frequently used biomaterials such as PMMA. The peptides were bound to the polymer through an acrylamide function that served as an anchor.^[30]

Results

Integrin pattern of osteoblasts

The integrin patterns of primary human osteoblasts, primary human osteoprogenitor cells, primary rat osteoblasts, and MC3T3-H1 mouse osteoblasts were investigated by fluorescence-activated cell sorting (FACS) analysis using antibodies labeled with fluorescein isothiocyanate (FITC) (LM 609 for $\alpha_v\beta_3$ integrin, P1F6 for $\alpha_v\beta_5$ integrin). Figure 1 shows $\alpha_v\beta_3$ and

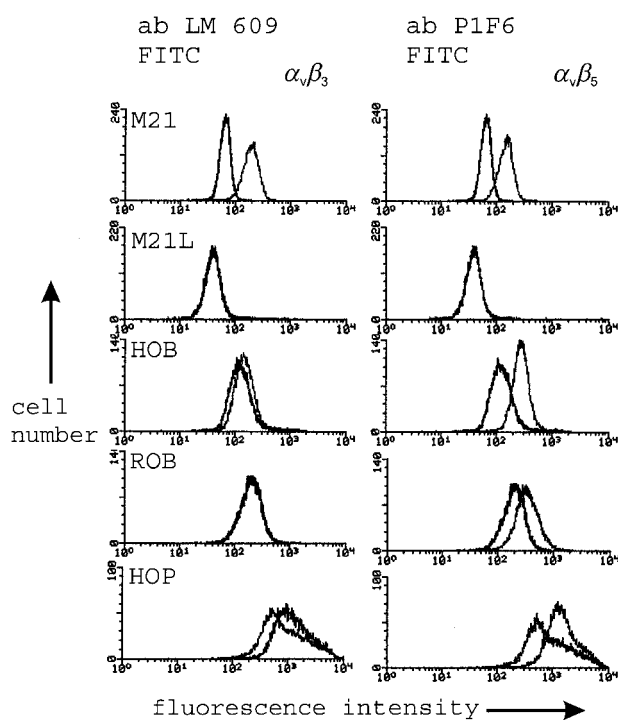


Figure 1. $\alpha_v\beta_3$ and $\alpha_v\beta_5$ integrin expression of different osteoblast cell cultures determined by FACS analysis with two different antibodies (antibody (ab) LM 609 = anti- $\alpha_v\beta_3$, ab P1F6 = anti- $\alpha_v\beta_5$). The following osteoblast cultures were used: M21 (human melanoma cell culture, $\alpha_v\beta_3$ - and $\alpha_v\beta_5$ -positive control cell culture), M21L (human melanoma cell culture, α_v -deficient, $\alpha_v\beta_3$ - and $\alpha_v\beta_5$ -negative control cell culture), HOB (primary human osteoblasts), ROB (primary rat osteoblasts), and HOP (primary human osteoprogenitor cells).

$\alpha_v\beta_3$ integrin expression by osteoblasts. Hence, the osteoblast cultures used in this study should be able to bind the $\alpha_v\beta_3$ - and $\alpha_v\beta_5$ -selective integrin ligand c(-RGDFK-).

Osteoblast-binding properties of surface-bound c(-RGDFK-)

For the first osteoblast-binding studies, maleimide-functionalized BSA surfaces were grafted with two thiol-modified derivatives of c(-RGDFK-) (Figure 2). Peptide **P1** contains a (3-mercaptopropyl)amide linker (\rightarrow 1) and peptide **P2** a succinyl

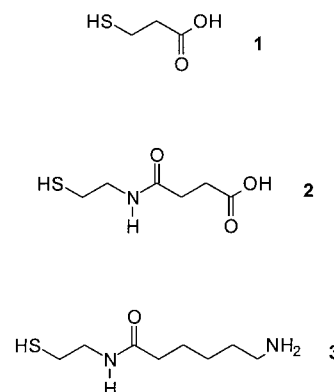


Figure 2. Different thiol linkers used for covalent linking of RGD cyclopeptides to BSA-coated surfaces. The linkers 1 and 2 are coupled to the highly active and selective ligand c(-RGDFK-), linker 3 to the weaker ligand c(-RGDEV-).

Editorial Advisory Board Member:^[*]

Horst Kessler,

born in Suhl, Thuringia, in 1940, studied chemistry at the universities of Leipzig and Tübingen. In 1966 he obtained his Ph.D. degree in Tübingen under Eugen Müller. He finished his habilitation in 1969 with studies on the detection of intramolecular mobility by NMR spectroscopy. In 1971 he became full professor of organic chemistry at the J. W. von Goethe University in Frankfurt. In 1989 he moved to the Technische Universität München. His main research interests are the conformationally oriented design and synthesis of biologically active molecules (peptides, sugars, peptidomimetics) and the development of NMR-spectroscopic techniques and their application to the study of biomolecules, especially peptides and proteins.



[*] Members of the Editorial Advisory Board will be introduced to the readers with their first manuscript.

cysteamide linker ($\rightarrow 2$). Both peptides stimulate binding of primary human osteoblasts, primary human osteoprogenitor cells, primary rat osteoblasts, and MC3T3-H1 mouse osteoblasts to the BSA surfaces (Figures 3–5). The cell adhesion rate

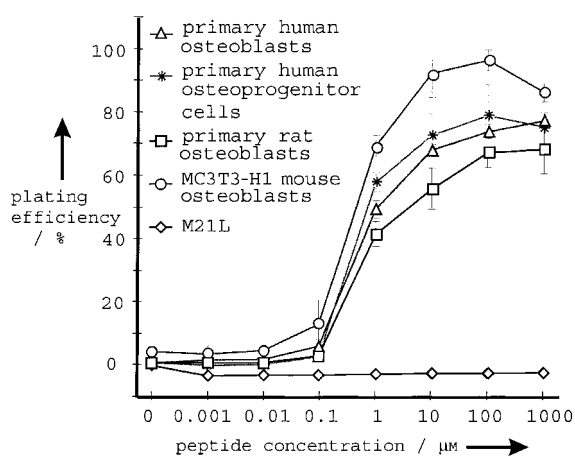


Figure 3. Dependence of the cell adhesion rate of different osteoblast cultures on the amount of peptide (thiol peptide P1 with c(RGDfK-) as the ligand) in the coating solution. M21L human melanoma cells, which do not express $\alpha_v\beta_3$ or $\alpha_v\beta_5$ integrin receptors, do not bind to the surface.

(expressed as a percentage; ratio of the number of adherent cells $\times 100$ to the number of seeded cells) increases with the peptide concentration in the coating solution. Encouraging values of 70–100% adhesion, depending on the osteoblast type, were obtained by using peptide concentrations of $> 10 \mu\text{M}$ with about 50 000 seeded cells per cm^2 of surface. Furthermore, cyclopeptide c(RGDEv-) ($v = \text{D-valine}$) containing linker 3 (P3), that is, an aminohexanoic acid spacer and a cysteamine anchor (Figure 2) at the glutamic acid residue, was synthesized. The only difference between this compound and the peptide used for grafting BSA surfaces in other studies^[10] is the cysteamine anchor instead of a cysteinamide anchor. This modification should not have any effect on the activity of the RGD cyclus but is essential for receiving a linker comparable to linkers 1 and 2. Figure 4 shows that c(RGDfK-) is much more effective in binding osteoblasts to BSA surfaces than c(RGDEv-). Receptor-binding studies with soluble integrins demonstrated that c(RGDfK-) is a stronger ligand for the $\alpha_v\beta_3$ and $\alpha_v\beta_5$ integrin receptors by a factor of 5 and 3, respectively, than c(RGDEv-).

To prove the validity of the cell-binding assay the melanoma cell line M21L was used as a negative control. The reason for the use of M21L cells is their deficiency in the expression of α_v receptors. As these melanoma cells show no cell-binding capacity at all on surfaces coated with α_v -selective RGD peptide (Figure 3), it can be concluded that the observed cell

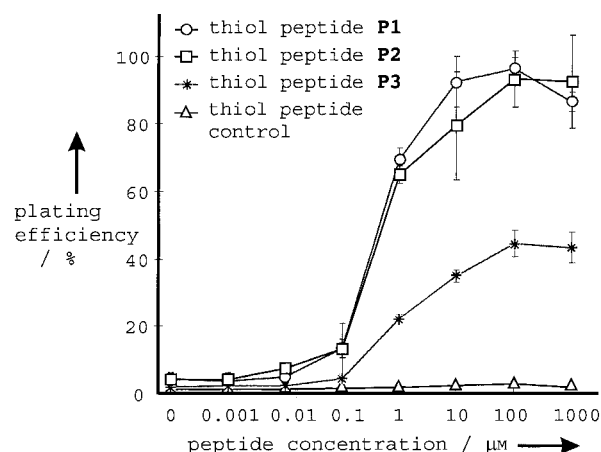


Figure 4. Effect of peptide sequence and linker length on the adhesion of MC3T3-H1 mouse osteoblasts. The thiol peptides P1 and P2 contain c(RGDfK-) as a highly active and selective integrin antagonist, thiol peptide P3 contains c(RGDEv-) as a ligand, the thiol peptide control contains β -alanine instead of glycine [$\rightarrow \text{c(R}(\beta\text{A)DfK-}$)] and is inactive.

adhesion phenomena in this system are completely dependent on the selective peptide and are not affected by other non-specific cell-binding processes. To prove that the cell adhesion is mediated by c(RGDfK-), the osteoblasts were pretreated with dissolved c(RGDfK-). They could be inhibited from binding to the surface depending on the concentration of the dissolved peptide (Figure 6). Additionally, as a negative control, BSA surfaces were coated with the control peptide c(R(β A)DfK-), in which the introduction of a single methylene group (β -alanine substitution for glycine) eliminates any binding activity towards the α_v integrin receptors. As expected, no cell adhesion was observed in this case (Figure 4).

Coating of PMMA surfaces with c(RGDfK-)

Coating of PMMA surfaces with $\alpha_v\beta_3$ -/ $\alpha_v\beta_5$ -selective integrin ligands was achieved by functionalization of c(RGDfK-) with

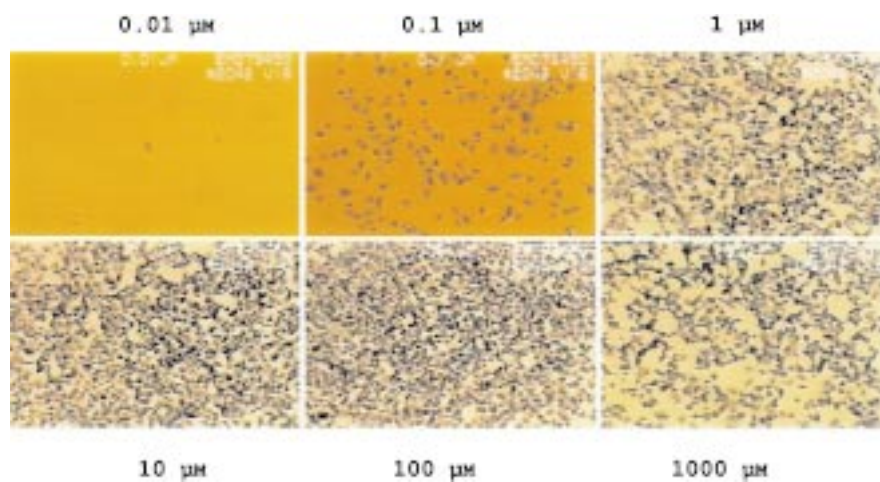


Figure 5. Optical microscopy image of MC3T3-H1 mouse osteoblasts (dark) attached on BSA surfaces that were coated with thiol peptide P1. The peptide concentration in the coating solution was between 0.01 and 1000 μM .

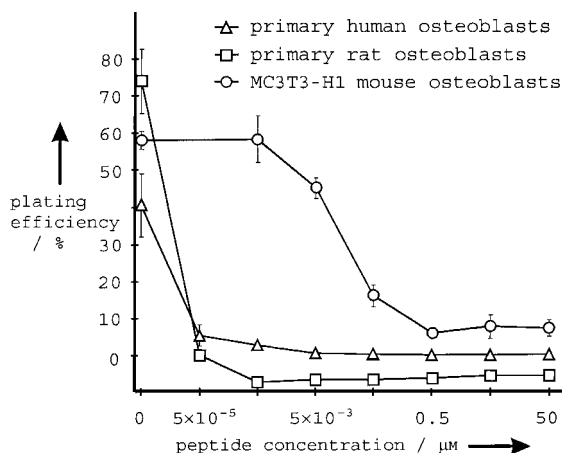


Figure 6. Dose-dependent inhibition of osteoblast binding to surfaces coated with thiol peptide P1 by dissolved c(RGDfK-) in various concentrations.

various-linker molecules containing an acrylamide anchor (Figure 7). These peptides were attached onto PMMA surfaces with camphorquinone. The coated surfaces were washed several times before treating with cells. PMMA bone cement was coated

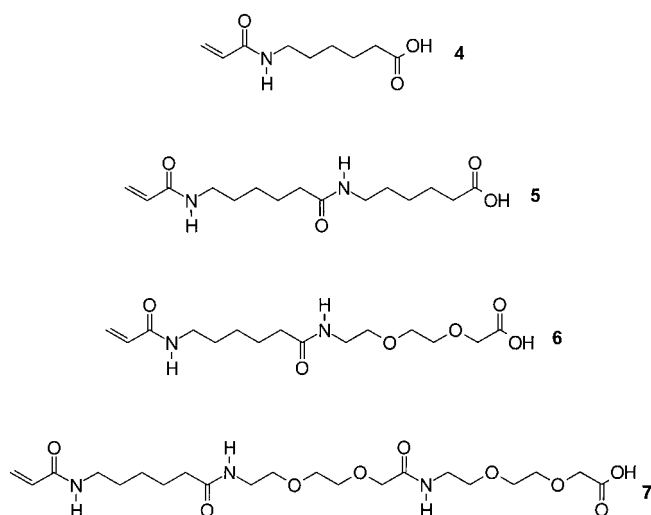


Figure 7. Different acrylamide linkers used for linking peptides to PMMA surfaces. They differ in length as well as in their hydrophilicity/hydrophobicity profile.

with a peptide containing aminohexanoic acid as a spacer between the RGD cyclus and acrylic acid (Figure 7), but these surfaces did not bind osteoblasts (Figure 8). It was therefore concluded that the distance between the PMMA surface and the RGD-binding sequence was too small for an integrin-mediated binding of cells to the c(RGDfK-) ligand. Thus, three peptides containing longer spacers with different lipophilicity/hydrophilicity profiles were synthesized (Figure 7): One spacer contains two aminohexanoic acid residues, the other two spacers contain only one aminohexanoic acid residue but additionally one or two triethylene glycol aminocarboxylic acid residues.

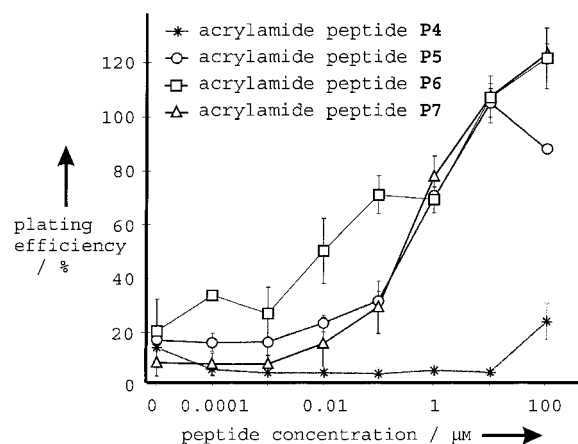


Figure 8. Effect of linker length on binding of MC3T3-H1 mouse osteoblasts to acrylamide peptides bound to PMMA. Different acrylamide peptides were tested which differ only in the nature of the linker (see Figure 7). Linker 4 is too short for adhesion of osteoblasts.

The latter two spacer types were used to introduce a hydrophilic glycol moiety close to the peptide to avoid a hydrophobic adhesion of the whole spacer to the polymer. Bone cement PMMA surfaces coated with any of these three peptides bind MC3T3-H1 mouse osteoblasts very effectively (Figure 8). A significant difference in cell-binding capacity between these three compounds was not observed. Analogous to the thiol peptides, cell adhesion rates of 100% could be achieved by using peptide concentrations of $> 10 \mu\text{M}$ with about 50000 seeded cells per cm^2 of surface. The adherent osteoblasts were tightly bound to the surface and could not be removed by washing or shaking. Figure 9 shows an optical microscopy image of MC3T3-H1 mouse osteoblasts adhered to PMMA surfaces coated with c(RGDfK-). It is obvious that the osteoblasts adhere poorly to noncoated PMMA surfaces. Cells attached to coated surfaces are forming focal adhesions and are stretched at the



Figure 9. Optical microscopy image of MC3T3-H1 mouse osteoblasts (dark) attached on uncoated PMMA surfaces (top) and on PMMA bone cement treated with acrylamide peptide P6 (bottom). The peptide concentration in the coating solution was $100 \mu\text{M}$. While the lower image is representative for the coated surface, the upper image shows the only area of the untreated surface where cell adhesion was observed at all.

surface in a typical manner, whereas the shape of cells attached to noncoated surfaces is spherical. Observing surface-bound osteoblasts over a period of 22 d, it was found that the adherent cells proliferated during this time, whereas cells not bound to surfaces died after a few days. Figure 10 shows the proliferation rate of adherent osteoblasts over a 22 d period. After this time, the number of osteoblasts has increased by a factor of 10, so that the PMMA surface is completely covered.

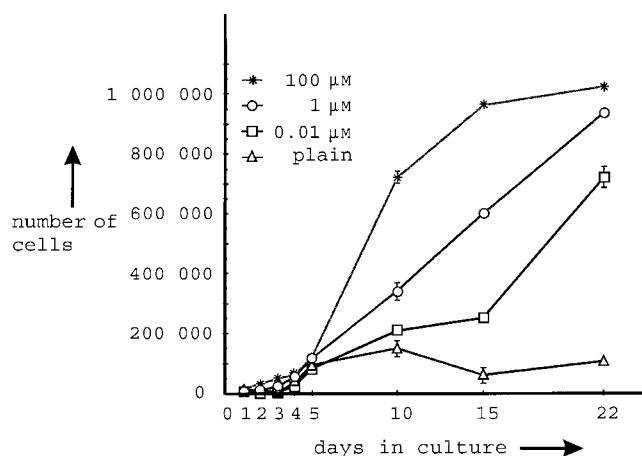


Figure 10. Stimulated proliferation of PMMA-attached MC3T3-H1 mouse osteoblasts over a time span of 22 d as a function of ligand density (acrylamide peptide P6) on the surface compared to an untreated control surface.

The osteoblast phenotype of the osteoblast cultures was proven by the differentiation markers alkaline phosphatase (histochemical enzyme assay) and by expression of collagen type I (immunofluorescence).

Animal studies with a rabbit model showed an induction of enhanced and accelerated cancellous bone ingrowth for the RGD-peptide-coated porous implants. Newly formed bone directly contacts the implant surface, and in fact an ingrowth of bone tissue towards the center of the porous implant was visible (Figure 11 A). In contrast, uncoated implants were separated from newly formed bone by a fibrous tissue layer (Figure 11 B), which prevented the formation of a direct implant–bone bonding.

Discussion

The thiol peptides P1 and P2 are much more effective in binding osteoblasts to BSA surfaces than the thiol peptide P3.^[10] This was expected as cyclic RGD peptides possess different activities and selectivities towards specific integrin receptor subtypes. It is well established that D-amino acids induce preferred conformations when they are incorporated into a cyclic peptide. RGD pentapeptides in which the D-amino acid follows Asp induce a conformation of the RGD sequence that is best recognized by $\alpha_v\beta_3$ and $\alpha_v\beta_5$ integrins. Additionally, a hydrophobic residue in this position, such as Phe, contributes to activity and selectivity. Therefore, c(-RGDEV-) is expected to be a weaker binder than c(-RGDFK-) in any application that involves binding to $\alpha_v\beta_3$ or $\alpha_v\beta_5$ integrins. This was proven by comparing the binding

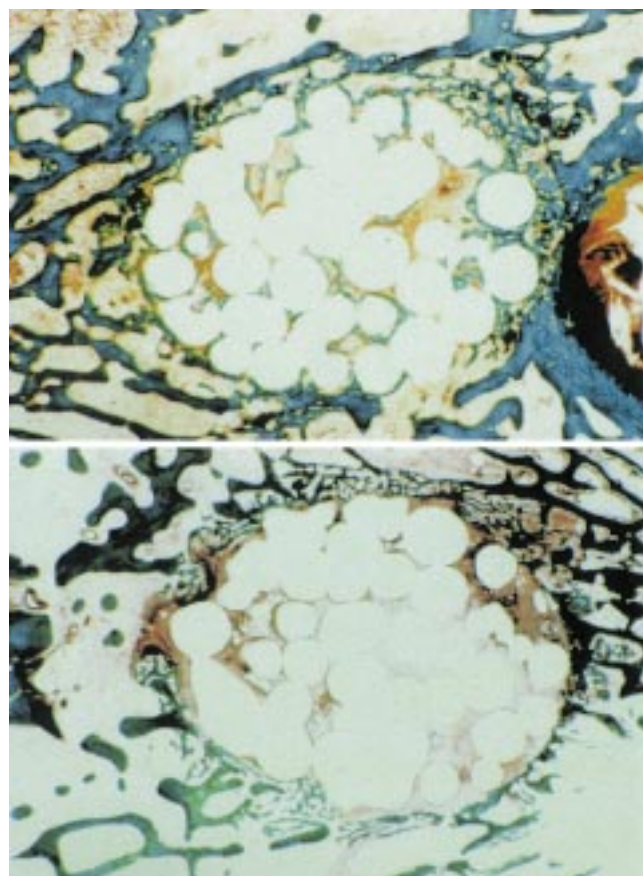


Figure 11. Cross-section of implanted PMMA implants (staining according to Goldner-Masson^[52]). Top: RGD-peptide-coated PMMA implant (magnification 16 ×). Bottom: Uncoated PMMA implant (magnification 16 ×). Color index: white: PMMA beads; green–blue: already existing bone and newly formed bone (visible in the top image around the PMMA beads), light brown: newly formed osteoid, a bone precursor, dark brown: fibrous tissue.

activities of c(-RGDFK-) and c(-RGDEV-) towards isolated $\alpha_v\beta_3$ and $\alpha_v\beta_5$ integrins: c(-RGDFK-) binds more strongly to $\alpha_v\beta_3$ and $\alpha_v\beta_5$ integrins by a factor of 5 and 3, respectively, than c(-RGDEV-).

For coating BSA surfaces with thiol peptides or PMMA surfaces with acrylamide peptides, a critical minimum distance of about 3.5 nm between surface and RGD pharmacophore was found to be essential for effective cell adhesion. The hydrophilicity/hydrophobicity profile of the spacer has no significant influence as the peptide with the linker 5 binds osteoblasts nearly as well as the peptides with the linkers 6 or 7 (Figure 8). Analysis of the cell adhesion rates as a function of the peptide concentration (Figures 3, 5, 8) shows a sigmoidal shape for all curves. Therefore, it can be concluded that there is a critical minimum density of integrin ligands bound to the surface below which no cell adhesion can be observed. Beyond the minimum density a direct dose-dependent increase of cell adhesion with the ligand density can be observed until the maximum value of 100% is reached (values above 100% are due to errors in the measurement). The slight decrease in cell binding at high ligand coatings may result from a negative effect of neighboring ligands on binding.

The observation that osteoblasts bound to the surface also proliferate, whereas suspended cells die within a few hours, confirms previous observations by Chen et al.^[31] They proved that integrin-mediated cell adhesion to surfaces can suppress apoptosis when the surface is large enough to allow cells to spread. If the surface area is too small, cells die even if they are adherent. In the experiments reported here no spatial limitation for cell spreading exists, and apoptosis is prevented.

As shown in the animal studies, the use of tailor-made RGD peptides is an attractive strategy for generating implants with a special biological information. This strategy is not only useful for bone replacements, it might also be an important contribution to tissue engineering.

Conclusion

A simple but very efficient method for the biofunctionalization of PMMA surfaces has been developed. This technique can find medical applications in the development of modern implants to prevent host-versus-graft reactions. In contrast to other techniques in which surfaces are coated with whole proteins, small highly active and selective cyclic peptides that contain the RGD-binding sequence in the bioactive conformation were used for coating. The peptides chosen exhibit highest activity for $\alpha_v\beta_5$ and $\alpha_v\beta_3$ integrin binding and have a very low affinity for the $\alpha_{IIb}\beta_3$ integrin. They were covalently bound to PMMA surfaces through an acrylamide anchor and bind osteoblasts selectively by interactions with their integrin receptors. In vitro, osteoblasts tightly attach to coated surfaces and proliferate, thereby forming a homogeneous cell layer at the polymer surface. In vivo, PMMA pellets coated with c-(RGDfK-) are integrated faster and more strongly into regenerating bone tissue of rabbits than uncoated pellets. These results demonstrate an attractive strategy for the development of cell-free and bioactive implants that carry the biological information for the selective activation of those target cells that are needed for selective tissue regeneration.

Experimental Section

General: Amino acids and coupling reagents were purchased from Novabiochem, 9-Fluorenylmethoxycarbonyl(Fmoc)-[2-(2-aminoethoxy)ethoxy]acetic acid from PerSeptive Biosystems, and solid-phase resin from Pepchem. All other chemicals were purchased from Aldrich, Sigma, or Fluka. Semipreparative HPLC was performed on a Beckmann instrument (system gold, solvent delivery module 126, UV detector 166) using a YMC ODS 120-5C18 column (5 μm , 20 \times 250 mm), with a flow rate of 6 mL min⁻¹. The eluant was 0.1% trifluoroacetic acid (TFA) in various acetonitrile–water gradients. HPLC–MS analyses were performed on a Hewlett Packard Series HP 1100. A YMC ODS-A 120-3C18 column (3 μm , 2 \times 125 mm) with a flow rate of 0.2 mL min⁻¹ and a Macherey & Nagel CC 125/2 Nucleosil 100-5C18 column (5 μm , 2 \times 125 mm) with a flow rate of 0.3 mL min⁻¹ were used. The eluant was 0.1% formic acid in an acetonitrile–water gradient (10 \rightarrow 50% acetonitrile in water over 15 min). ESI-MS measurements were performed on a Finnigan LCQ instrument. NMR spectra were recorded with a Bruker AC250 spectrometer.

Peptide synthesis

Cyclic peptides: The cyclic peptides were synthesized by a combined solid-phase–solution methodology: Linear peptides were synthesized by using the Fmoc strategy^[32] on tritylchloride–polystyrene (TCP) resin.^[33, 34] Amino acids were coupled stepwise with *O*-(1*H*-benzotriazol-1-yl)-*N,N,N'*-tetramethyluronium tetrafluoroborate (TBTU) and 1-hydroxybenzotriazole (HOBT) as coupling reagents. Permanent protecting groups were 4-methoxy-2,3,6-trimethylbenzolsulfonyl (Mtr) for Arg, *tert*-butyl (tBu) for Asp, and benzyloxycarbonyl (Z) for Lys and Glu. Cyclization of the linear peptides was performed in solution with diphenylphosphoryl azide (DPPA)^[35, 36] and NaHCO₃.

Thiol peptides: Reaction of c-(R(Mtr)GD(OtBu)fK-) with succinic anhydride followed by coupling of 5-tritylcysteamine^[37] with *N*-ethyl-*N,N'*-(dimethylaminopropyl)carbodiimide hydrochloride (EDCI·HCl) and deprotection with TFA/H₂O/1,2-ethanedithiol (90:5:5) yielded the thiol peptide **P1**,^[37] reaction of c-(R(Mtr)GD(OtBu)fK-) with *N*-succinimidyl-5-tritylmercaptopropionate followed by analogous deprotection yielded the thiol peptide **P2**.^[37] Both peptides were purified by HPLC. 5-trityl-protected thiol linker **3** was synthesized using standard procedures of peptide chemistry.^[38] Analytical data for **3**: ¹H NMR (250 MHz, [D₆]DMSO, 27 °C): δ = 7.45–7.10 (m, 15 H; Trt), 5.55 (m, 1 H; NH), 3.05 (q, ³J(H,H) = 6 Hz, 2 H; CH₂-NHCO), 2.65 (t, ³J(H,H) = 7 Hz, 2 H; CH₂-N), 2.35 (t, ³J(H,H) = 6 Hz, 2 H; CH₂-S), 2.05 (t, 2 H; CH₂-CONH), 1.80 (s, 2 H; NH₂), 1.65–1.25 (m, 6 H; (CH₂)₃-); MS (ESI): *m/z* (%): 243.1 (100) [Trt]⁺, 433.0 (5) [M+H]⁺, 455.1 (7) [M+Na]⁺. **3** was coupled to c-(R(Mtr)GD(OtBu)Ev-) with EDCI·HCl. Purification by HPLC, deprotection with TFA/H₂O/1,2-ethanedithiol (90:5:5), and further purification by HPLC yielded thiol peptide **P3**. Analytical data for **P3**: HPLC–MS (ESI): *m/z* (%): 365.6 (22) [M+2H]²⁺, 384.6 (7) [M+H+K]²⁺, 729.6 (100) [M+H]⁺, 751.6 (8) [M+Na]⁺, 767.5 (5) [M+K]⁺.

Acrylamide peptides: The linkers **4** and **5** were synthesized in solution according to Pless et al.^[39] The linkers **6** and **7** were synthesized by solid-phase synthesis using the Fmoc strategy coupling linker **4** as the last building block. The ¹H NMR data of linker **4** agree with those reported in the literature.^[39] Analytical data for **5–7**: **5**: ¹H NMR (250 MHz, [D₆]DMSO, 27 °C): δ = 8.03 (m, 1 H; NH), 7.70 (m, 1 H; NH), 6.16 (dd, ³J(H,H) = 17, 10 Hz, 1 H; =CH), 6.03 (dd, ²J(H,H) = 17 Hz, ²J(H,H) = 2.5 Hz, 1 H; CH₂=), 5.53 (dd, ³J(H,H) = 10 Hz, ²J(H,H) = 2.5 Hz, 1 H; CH₂=), 3.15–2.95 (m, 4 H; N-CH₂), 2.17 (t, ³J(H,H) = 7 Hz, 2 H; CH₂-COO), 2.02 (t, ³J(H,H) = 7 Hz, 2 H; CH₂-CON), 1.55–1.15 (m, 12 H; (CH₂)₃); MS (ESI): *m/z* (%): 299.2 (17) [M+H]⁺, 321.2 (97) [M+Na]⁺, 337.2 (100) [M+K]⁺. **6**: ¹H NMR (250 MHz, CDCl₃, 27 °C): δ = 6.87 (m, 1 H; NH), 6.43 (m, 1 H; NH), 6.25 (dd, ³J(H,H) = 17 Hz, ²J(H,H) = 2 Hz, 1 H; CH₂=), 6.11 (dd, ³J(H,H) = 17, 10 Hz, 1 H; =CH=), 5.62 (dd, ³J(H,H) = 10 Hz, ²J(H,H) = 2 Hz, 1 H; CH₂=), 4.12 (s, 2 H; O-CH₂-COO), 3.73–3.23 (m, 10 H; CH₂-CH₂-O, N-CH₂), 2.22 (t, ³J(H,H) = 7 Hz, 2 H; CH₂-CON), 1.70–1.27 (m, 6 H; (CH₂)₃); MS (ESI): *m/z* (%): 331.2 (100) [M+H]⁺. **7**: ¹H NMR (250 MHz, CDCl₃, 27 °C): δ = 7.30 (m, 2 H; NH), 6.67 (m, 1 H; NH), 6.25 (dd, ³J(H,H) = 17 Hz, ²J(H,H) = 2 Hz, 1 H; CH₂=), 6.11 (dd, ³J(H,H) = 17, 10 Hz, 1 H; CH=), 5.62 (dd, ³J(H,H) = 10 Hz, ²J(H,H) = 2 Hz, 1 H; CH₂=), 4.13 (s, 2 H; O-CH₂-COO), 3.99 (s, 2 H; O-CH₂-CON), 3.80–3.25 (m, 18 H; CH₂-CH₂-O, N-CH₂), 2.20 (t, ³J(H,H) = 7 Hz, 2 H; CH₂-CON), 1.75–1.27 (m, 6 H; (CH₂)₃); MS (ESI): *m/z* (%): 476.2 (100) [M+H]⁺, 498.3 (60) [M+Na]⁺, 514.3 (21) [M+K]⁺. The linkers were coupled to c-(R(Mtr)GD(OtBu)fK-) in solution with *O*-(7-azabenzotriazol-1-yl)-*N,N,N'*-tetramethyluronium hexafluorophosphate (HATU), 1-hydroxy-7-azabenzotriazole (HOAt), and collidine. The resulting acrylamide peptides **P4–P7** were purified by HPLC and deprotected with TFA/H₂O (95:5). Analytical data for acrylamide peptides **P4–P7**: **P4**: HPLC–MS (ESI): *m/z* (%): 771.4 (100) [M+H]⁺, 793.4 (8) [M+Na]⁺, 809.3 (5) [M+K]⁺. **P5**: HPLC–MS (ESI): *m/z* (%):

884.7 (100) [M+H]⁺, 906.5 (7) [M+Na]⁺. **P6:** HPLC–MS (ESI): *m/z* (%): 916.5 (100) [M+H]⁺, 938.6 (7) [M+Na]⁺. **P7:** HPLC–MS (ESI): *m/z* (%): 1061.7 (100) [M+H]⁺, 1083.6 (7) [M+Na]⁺. All peptides were finally characterized by 1D ¹H NMR spectroscopy (250 MHz), and the expected spectra were obtained.

Receptor binding assays: Vitronectin and fibrinogen from human plasma were prepared as described by Mitjans et al.^[40] $\alpha_{\text{IIb}}\beta_3$ was purified from outdated thrombocytes,^[41] $\alpha_v\beta_3$ was obtained from term human placenta.^[42] The integrins were >95% pure as determined by SDS-PAGE and by an enzyme-linked immunosorbant assay (ELISA). Receptor inhibition assays were performed as described by Haubner et al.^[43]

Cell culture: Primary human osteoprogenitor cells were isolated from human bone marrow stromal cells as described by Vilamitjana-Amedee et al.^[44] The osteogenic potential of the cells was stimulated by addition of dexamethasone (10⁻⁸ M) to the culture medium (culture conditions: Iscove's modified Dulbecco's medium (IMDM), 10% fetal calf serum (FCS); humidified atmosphere, 10% CO₂, 37 °C). Primary human osteoblasts were kindly provided by Siggelkow et al.^[45] (culture conditions: Dulbecco's modified Eagle medium (DMEM), 58.5 µg mL⁻¹ glutamine, 10% FCS; humidified atmosphere, 5% CO₂, 37 °C). Primary rat osteoblasts were isolated according to Yagiela and Woodbury^[46] (culture conditions: DMEM, 58.5 µg mL⁻¹ glutamine, 100 µg mL⁻¹ penicillin, 100 µg mL⁻¹ streptomycin, 10% FCS; humidified atmosphere, 5% CO₂, 37 °C). Mouse calvaria osteoblastic cells of the line MC3T3-H1 were kindly provided by Heermeier et al.^[47] (culture conditions: DMEM, 25 mM 2-[4-(2-hydroxyethyl)-1-piperazinyl] ethanesulfonic acid (HEPES), 100 µg mL⁻¹ penicillin, 100 µg mL⁻¹ streptomycin, 10% FCS; humidified atmosphere, 5% CO₂, 37 °C). Human melanoma cells of the line M21L were kindly provided by Cheresch et al. (culture conditions: Rosswel Park Memorial Institute (RPMI) 1640 medium, 10% FCS, 2 mM L-glutamine, and 50 µg mL⁻¹ gentamicin; humidified atmosphere, 7.5% CO₂, 37 °C). The human melanoma cell line M21 is a polyclonal line isolated from lymph nodes and the M21L cell line is an α_v -deficient M21 subpopulation called M21 Low. All cell culture components were ordered from GIBCO (UK).

Analysis of cellular integrin expression: The integrin expression patterns of the different osteogenic cells were measured with a Becton–Dickinson fluorescence-activated cell sorter (FACS). The cells were adjusted to 1 × 10⁶ cells mL⁻¹, washed twice with 1% (w/v) BSA in phosphate-buffered saline (PBS), and analyzed by using fluorescently labeled antibodies against $\alpha_v\beta_3$ integrin (ab LM 609,^[48] isolated from mouse ascites and kindly provided by Dr. D. A. Cheresch, The Scripps Research Institute, La Jolla, USA) and $\alpha_v\beta_5$ integrin (ab P1F6, isolated from mouse ascites and kindly provided by Merck KGaA).

RGD peptide coatings: The covalent coating of the thiol peptides onto BSA-coated cell culture plates (48 wells) was carried out according to Ruoslahti et al.^[49] Peptides were diluted from 10³ µM to 10⁻³ µM and linked to BSA with sulfosuccinimidyl 4-(*p*-maleimidophenyl)butyrate (Pierce) in a concentration of 1 µg mL⁻¹. The covalent grafting of prepolymerized PMMA discs with peptides was performed by incubation with a solution of the acrylamide peptide in DMSO and successive addition of isopropyl alcohol with 0.2% (w/v) camphorquinone at peptide concentrations ranging from 10² µM to 10⁻⁴ µM under UV radiation for 2 h.

Cell adhesion assay: The cell adhesion assays were performed as described by Landegren et al.^[50] Osteoblasts were seeded on the substrate at a density of 50 000 cells per well. The cells were allowed to adhere for 1 h under standard tissue culture conditions (i. e., 37 °C, 5% CO₂) in culture medium containing 1% BSA (w/v). After another 2 h the wells were washed three times with PBS (pH 7.4) to remove

nonadherent cells. Attached cells were quantified by an ELISA detecting the lysosomal enzyme hexosaminidase. The amount of colored product was measured with an ELISA reader (SLT Rainbow) at 405 nm. Results are given as the percentage of the total number of cells seeded (which is considered as 100% of cell adhesion), which is defined as the plating efficiency. For competitive cell adhesion assays, the cells were preincubated with dissolved RGD peptides of different concentrations for 15 min and then incubated on the RGD-peptide-coated surface as described above. In all experiments, the mean value of each point given in the figures is the result of triplicate determinations, the error bars represent standard deviations. The number of identical but independent in vitro experiments was at least three.

Cell proliferation assay: Proliferation was observed by using the WST-1 colorimetric test, which measures mitochondrial dehydrogenase activity by formazan reaction. 12 500 cells per well were seeded under serum-free conditions (DMEM, 25 mM HEPES, 0.1% BSA (w/v) in PBS) on the different surfaces. After 2 h of treatment under standard culture conditions the cells were washed three times to remove nonadherent cells. Discs were then cultured for 22 d. Exchange of culture medium was carried out routinely every 3 d. The first measurement was done after 24 h. The test was performed as described by Hamasaki et al.^[51] The osteogenic cells were incubated with WST-1 reagent for 4 h at 37 °C. The colored product was measured over a period of 22 d (on day 1, 2, 3, 4, 5, 10, 15, 22) at 450 nm using an ELISA reader (SLT Rainbow). The osteoblast phenotype of the osteoblast cultures was proven by the differentiation markers alkaline phosphatase (histochemical enzyme assay) and by expression of collagen type I (immunofluorescence). In all experiments, the mean value of each point given in the figures is the result of triplicate determinations, the error bars represent standard deviations. The number of identical but independent in vitro experiments was at least three.

Animal studies: A rabbit model was used for the animal studies. PMMA implants (8 mm length, 4.6 mm diameter) were made of hard tissue repair material (HTR; Walter Lorenz, Jacksonville, USA) glued with monomethyl methacrylate to build interconnective porosity. RGD-peptide-coated and -uncoated control PMMA implants were with direct contact to bone (press-fit implantation) implanted into the patella groove with the diamond bone cutting system (DBCS) from Merck Biomaterial GmbH (Germany). After two weeks the implants were removed, and newly formed bone was examined by analyzing cross-sections with a histological staining method according to Goldner-Masson.^[52] The animal study results represent six implants of each group in six animals.

The authors thank B. Blessing, G. Fleißner, H.-G. Kreysch, M. Wolff, M. Kranawetter, and B. Cordes for technical assistance, and T. Malia for careful reading of the manuscript.

- [1] J. A. Eble in *Integrin–Ligand Interaction* (Ed.: J. A. Eble), Springer, Heidelberg, **1997**, pp. 1–40.
- [2] K. Kühn in *Integrin–Ligand Interaction* (Ed.: J. A. Eble), Springer, Heidelberg, **1997**, pp. 41–83.
- [3] S. Dedhar, *Curr. Opin. Hematol.* **1999**, *6*, 37–43.
- [4] A. Howe, A. E. Aplin, S. K. Alahari, R. L. Juliano, *Curr. Opin. Cell Biol.* **1998**, *10*, 220–231.
- [5] N. J. Boudreau, P. L. Jones, *Biochem. J.* **1999**, *339*, 481–488.
- [6] F. G. Giancotti, E. Ruoslahti, *Science* **1999**, *285*, 1028–1032.
- [7] S. M. Schoenwaelder, K. Burridge, *Curr. Opin. Cell Biol.* **1999**, *11*, 274–286.
- [8] J. Lahann, D. Klee, H. Klint, A. Ince, H. Höcker, J. Reul, *Proceedings of the 24th Annual Meeting of the Society for Biomaterials*, San Diego, USA, **1998**, p. 136.

- [9] J. R. Glass, W. S. Craig, K. Dickerson, M. D. Pierschbacher, *Mat. Res. Soc. Proc.* **1992**, 252, 331–337.
- [10] D. Delforge, M. Art, B. Gillon, M. Dieu, E. Delaive, M. Raes, J. Remacle, *Anal. Biochem.* **1996**, 242, 180–186.
- [11] A. Rezania, C. H. Thomas, A. B. Branger, C. M. Waters, K. E. Healy, *J. Biomed. Mater. Res.* **1997**, 37, 9–19.
- [12] W. J. Kao, J. A. Hubbell, *Proceedings of the 23rd Annual Meeting of the Society for Biomaterials*, New Orleans, USA, **1997**, p. 4.
- [13] S. Kouvrakoglou, K. C. Dee, R. Bizios, L. V. McIntire, K. Zygourakis, *Proceedings of the 23rd Annual Meeting of the Society for Biomaterials*, New Orleans, USA, **1997**, p. 5.
- [14] Y. W. Tong, M. S. Shoichet, *Proceedings of the 23rd Annual Meeting of the Society for Biomaterials*, New Orleans, USA, **1997**, p. 7.
- [15] L. Kam, P. M. St. John, H. G. Craighead, M. Isaacson, J. N. Turner, W. Shain, R. Bizios, *Proceedings of the 23rd Annual Meeting of the Society for Biomaterials*, New Orleans, USA, **1997**, p. 8.
- [16] J. P. Bearinger, C. H. Thomas, K. E. Healy, *Proceedings of the 23rd Annual Meeting of the Society for Biomaterials*, New Orleans, USA, **1997**, p. 54.
- [17] R. F. Valentini, D. Ferris, C. DiGiovanni, P. Dimond, M. Sherling, G. Moodie, T. Crisco, D. Labrador, M. Ehrlich, *Proceedings of the 23rd Annual Meeting of the Society for Biomaterials*, New Orleans, USA, **1997**, p. 55.
- [18] K. C. Dee, T. T. Andersen, R. Bizios, *Proceedings of the 23rd Annual Meeting of the Society for Biomaterials*, New Orleans, USA, **1997**, p. 60.
- [19] T. Pakalns, K. Haverstick, Y. C. Yu, G. B. Fields, J. B. McCarthy, M. Tirrell, *Proceedings of the 23rd Annual Meeting of the Society for Biomaterials*, New Orleans, USA, **1997**, p. 221.
- [20] A. Rezania, R. W. Johnson, K. E. Healy, *Proceedings of the 23rd Annual Meeting of the Society for Biomaterials*, New Orleans, USA, **1997**, p. 222.
- [21] K. Haverstick, P. Berndt, Y. C. Yu, T. Pakalns, J. Schneider, G. Fields, M. Tirrell, *Proceedings of the 23rd Annual Meeting of the Society for Biomaterials*, New Orleans, USA, **1997**, p. 223.
- [22] K. C. Dee, T. T. Andersen, R. Bizios, *Proceedings of the 23rd Annual Meeting of the Society for Biomaterials*, New Orleans, USA, **1997**, p. 228.
- [23] D. L. Hern, J. A. Hubbell, *J. Biomed. Mater. Res.* **1998**, 39, 266–276.
- [24] C. Roberts, C. S. Chen, M. Mrksich, V. Martichonok, D. E. Ingber, G. M. Whitesides, *J. Am. Chem. Soc.* **1998**, 120, 6548–6555.
- [25] M. Aumailley, M. Gurrath, G. Müller, J. Calvete, R. Timpl, H. Kessler, *FEBS Lett.* **1991**, 291, 50–54.
- [26] G. Müller, M. Gurrath, H. Kessler, R. Timpl, *Angew. Chem.* **1992**, 104, 341–343; *Angew. Chem. Int. Ed. Engl.* **1992**, 31, 326–328.
- [27] M. Pfaff, K. Tangemann, B. Müller, M. Gurrath, G. Müller, H. Kessler, R. Timpl, J. Engel, *J. Biol. Chem.* **1994**, 269, 20233–20238.
- [28] R. Haubner, R. Gratias, B. Diefenbach, S. L. Goodman, A. Jonczyk, H. Kessler, *J. Am. Chem. Soc.* **1996**, 118, 7461–7472.
- [29] R. Haubner, D. Finsinger, H. Kessler, *Angew. Chem.* **1997**, 109, 1440–1456; *Angew. Chem. Int. Ed.* **1997**, 36, 1374–1389.
- [30] M. Kantlehner, D. Finsinger, J. Meyer, P. Schaffner, A. Jonczyk, B. Diefenbach, B. Nies, H. Kessler, *Angew. Chem.* **1999**, 111, 587–590; *Angew. Chem. Int. Ed.* **1999**, 38, 560–562.
- [31] C. S. Chen, M. Mrksich, S. Huang, G. M. Whitesides, D. E. Ingber, *Science* **1997**, 276, 1425–1428.
- [32] G. B. Fields, R. L. Noble, *Int. J. Pept. Protein Res.* **1990**, 35, 161–214.
- [33] E. Bayer, N. Clausen, C. Goldammer, B. Henkel, W. Rapp, L. Zhang, *Proceedings of the 13th American Peptide Symposium*, Edmonton, Canada, **1994**, pp. 156–158.
- [34] B. Henkel, L. Zhang, C. Goldammer, E. Bayer, *Z. Naturforsch. B* **1996**, 51, 1339–1346.
- [35] T. Shiori, K. Ninomiya, S.-I. Yamada, *J. Am. Chem. Soc.* **1972**, 90, 6203–6205.
- [36] S. F. Brady, S. L. Varga, R. M. Freidinger, D. A. Schwenk, M. Mendlowski, F. W. Holly, D. F. Veber, *J. Org. Chem.* **1979**, 44, 3101–3105.
- [37] a) D. Finsinger, Dissertation, Technische Universität München, Germany, **1997**; b) A. Jonczyk, S. L. Goodman, B. Diefenbach, A. Sutter, H. Kessler (Merck), WO-A 97/14716, **1997** [*Chem. Abstr.* **1997**, 127(2), 17965].
- [38] M. Bodanszky, *Peptide Chemistry*, 2nd ed., Springer, Heidelberg, **1993**.
- [39] D. D. Pless, Y. C. Lee, S. Roseman, R. L. Schnaar, *J. Biol. Chem.* **1983**, 258, 2348–2349.
- [40] F. Mitjans, D. Sander, J. Adan, A. Sutter, J. M. Martinez, C. S. Jaggle, J. M. Moyano, H. G. Kreysch, J. Piulats, S. L. Goodman, *J. Cell. Sci.* **1995**, 108, 2825–2838.
- [41] R. Pytela, M. D. Pierschbacher, M. H. Ginsberg, E. F. Plow, E. Ruoslahti, *Science* **1986**, 231, 1559–1562.
- [42] a) J. W. Smith, D. A. Cheresch, *J. Biol. Chem.* **1988**, 263, 18726–18731; b) J. W. Smith, D. J. Vestal, S. V. Irwin, T. A. Burke, D. A. Cheresch, *J. Biol. Chem.* **1990**, 265, 11008–11013.
- [43] R. Haubner, W. Schmitt, G. Hölzemann, S. L. Goodman, A. Jonczyk, H. Kessler, *J. Am. Chem. Soc.* **1996**, 118, 7881–7891.
- [44] J. Vilamitjana-Amedee, R. Bareille, F. Rouais, A. I. Caplan, M. F. Harmand, *In Vitro Cell* **1993**, 29, 699–707.
- [45] H. Siggelkow, D. Hilmes, K. Rebenstorff, W. Kurre, I. Engel, M. Hüfner, *Clin. Chim. Acta* **1998**, 272, 111–125.
- [46] J. A. Yagiela, D. M. Woodbury, *Anat. Rec.* **1977**, 188, 287–295.
- [47] K. Heermeier, M. Spanner, J. Träger, R. Gradinger, J. Schmidt, *Cells Mater.* **1995**, 5, 309–321.
- [48] D. A. Cheresch, R. C. Spiro, *J. Biol. Chem.* **1987**, 262, 17703–17711.
- [49] E. Ruoslahti, E. G. Hayman, M. Pierschbacher, E. Engvall, *Methods Enzymol.* **1982**, 82, 803–831.
- [50] U. Landegren, *J. Immunol. Methods* **1984**, 67(2), 379–388.
- [51] K. Hamasaki, K. Kogure, K. Ohwada, *Toxicon* **1996**, 34(4), 490–495.
- [52] J. Goldner, *Am. J. Path.* **1938**, 14, 237–243.

Received: March 21, 2000 [F 23]